Biomechan Model Mechanobiol
DOI 10.1007/s10237-007-0115-9

ORIGINAL PAPER

Evolving mechanical properties of a model of abdominal aortic aneurysm

P. N. Watton · N. A. Hill

Received: 5 November 2007 / Accepted: 19 November 2007

Abstract The novel three-dimensional (3D) mathematical model for the development of abdominal aortic aneurysm (AAA) of Watton et al. Biomech Model Mechanobiol 3(2): 98–113, (2004) describes how changes in the micro-structure of the arterial wall lead to the development of AAA, during which collagen remodels to compensate for loss of elastin. In this paper, we examine the influence of several of the model's material and remodelling parameters on growth rates of the AAA and compare with clinical data. Furthermore, we calculate the dynamic properties of the AAA at different stages in its development and examine the evolution of clinically measurable mechanical properties. The model predicts that the maximum diameter of the aneurysm increases exponentially and that the ratio of systolic to diastolic diameter decreases from 1.13 to 1.02 as the aneurysm develops; these predictions are consistent with physiological observations of Vardulaki et al. Br J Surg 85:1674–1680 (1998) and Lanne et al. Eur J Vasc Surg 6:178–184 (1992), respectively. We conclude that mathematical models of aneurysm growth have the potential to be useful, noninvasive diagnostic tools and thus merit further development.

1 Introduction

Abdominal aortic aneurysm (AAA) is characterised by a bulge in the abdominal aorta. Development of AAA is associated with dilation of the arterial wall and the possibility of rupture; 80–90% of ruptured aneurysms will result in death (Wilmink et al. 1999). Surgery to remove the aneurysm is an option, but it is a high-risk procedure with a 5% mortality rate (Raghavan and Vorp 2000). Statistically, it is observed that the risk of rupture exceeds the risk of the operation when the diameter exceeds 5.5 cm (Powell and Brady 2004). However, this criterion fails to identify small aneurysms with high risk of rupture and large aneurysms with low risk. Thus there is a general need for improved diagnostic criteria to aid clinical decisions.

Several models have analysed the stress distributions in AAAs utilising idealised (Elger et al. 1996) or physiological geometries (Raghavan and Vorp 2000). These aim to yield an improved diagnostic tool for predicting rupture. However, a detailed knowledge of the AAA wall thickness and histology of the tissue needs to be non-invasively determined to successfully predict stresses (and the strength) of the aneurysmal tissue on a patient specific basis. Hence current state-of the-art biomechanical models of AAA are not ready for clinical application and patient management (Vorp 2007) and thus to date, rupture risk is still based on the diameter of an AAA.

Modelling growth of an aneurysm will ultimately lead to a greater understanding of the pathogenesis of the disease and may yield improved criteria for the prediction of rupture. However, we emphasize that growth models of AAA (Watton et al. 2004), and similarly intracranial cerebral aneurysms (Baek and Humphrey 2006; Kroon and Holzapfel 2007), still require significant development to realise clinical application.

In the healthy artery, the main load bearing constituents in the arterial wall are elastin and collagen. Collagen is considerably stiffer than elastin; however, at physiological strains elastin bears most of the load (Armentano et al. 1995). This is because collagen is tortuous in nature (Shadwick 1999;

P. N. Watton (✉)
Department of Engineering Science, University of Oxford,
Parks Road, Oxford OX1 3PJ, UK
e-mail: Paul.Watton@eng.ox.ac.uk

N. A. Hill
Department of Mathematics, University of Glasgow,
University Gardens, Glasgow G12 8QW, UK

Raghavan et al. 1999). In fact, at each point in unloaded tissue, there is a population of collagen fibrils which display varying degrees of undulation. It is only at physiological pressures that the fibrils begin to straighten out and contribute to load bearing (Sverdlik and Lanir 2002; Sacks 2003). The progressive recruitment of a population of fibrils gives rise to the highly nonlinear mechanical response of the collagen.

Several recent microstructural models of collagen describe the detailed behaviour of specimens of collagenous tissue under repeated loading in vitro. For example, Sverdlik and Lanir (2002) examined pre-conditioning of sheep digital tendons assuming that individual collagen fibrils have quasi-linear viscoelastic properties, while Sacks (2003) studied native bovine pericardium and took the fibrils to be linearly elastic and assumed that it is the progressive recruitment of a population of fibrils that gives rise to the highly nonlinear mechanical response of the collagenous tissue. In both these models, the waviness of individual fibrils in the tissue varies according to a probability density function, and the tissue stress–strain relationships are obtained by integrating over the population of fibrils. Such models often define the straightening stretch ratio (SSR) of each individual fibril (e.g. Sverdlik and Lanir 2002) and assume that the individual fibrils do not bear load until the undulation disappears. (Note though that Hansen et al. (2002) reports a small but detectable force whilst there is still an observable crimp). These models are complicated and require a number of parameters to be fitted to experimental data using statistical model sensitivity tests. Moreover these models do not address the changes in the tissue stress–strain relationship that arise when the tissue remodels in vivo. Hence we utilize a constitutive model (Holzapfel et al. 2000) that accounts for the gross mechanical response of the collagen.

Collagen is in a continual state of deposition and degradation with a relatively fast turnover of 3–90 days (Humphrey 1999). More specifically, Nissen et al. (1978) determined the collagen half-life of the aorta and mesenteric arteries of a rat to be 60–70 days in normotensive animals and reduced to 17 days in hypertensive conditions. The collagen fibres are secreted by fibroblasts. These cells work on the collagen, crawling over it and tugging on it in order to compact it into sheets and draw it out into cables. In doing this, the fibroblasts attach the collagen fibres to the extra-cellular matrix in a state of strain (Alberts et al. 1994, p. 984). This ensures that, at the higher end of the physiological range of pressures, collagen contributes to the load bearing of the arterial wall. The process of fibre deposition and degradation naturally acts to remodel the arterial wall in response to changing physiological conditions. The theoretical study by Humphrey (1999) has served as the foundation for a number of theoretical studies that address the remodelling of collagen in pathological conditions (Humphrey and Rajagopal 2002, 2003; Gleason et al. 2004; Gleason and Humphrey 2004, 2005; Baek and Humphrey 2006).

During the growth of an AAA, it is observed that there is an accompanying loss of elastin (He and Roach 1993). However, the degradation of elastin alone does not explain the large dilatations observed in aneurysms because the collagen is very stiff and has a strongly nonlinear tensile response curve. Therefore models of aneurysm growth must address both the degradation of elastin and the remodelling of collagen.

The unloaded artery (no internal pressure, no axial force) is not stress free. If a radial cut is made in the axial direction, it springs open into an approximate circular sector which is characterised by an opening angle which can be measured experimentally (Rachev and Greenwald 2003). This geometry is often adopted as the stress-free configuration. However, the geometry is not actually a circular sector and moreover the artery may still contain residual stresses. Consequently, two alternative hypotheses exist that enable an unstressed reference configuration to be defined. It may be hypothesised that the physiological state of a healthy artery has either:

(i) constant circumferential stress in each of its layers (Ogden and Schulze-Bauer 2000)
(ii) uniform strain distribution through the thickness of the wall. (Takamizawa and Hayashi 1987).

Although all the previous (three) hypotheses are not equivalent, they all yield stress and strain distributions through the thickness of the wall that are more uniform at physiological pressures than if the unloaded artery had been adopted as the stress-free reference configuration. For example, Stergiopulos et al. (2001) model the porcine aortic media as two stress free circular sectors and observe that the radial distribution of circumferential stretch is close to uniform with a difference between stretch ratios at the inner and outer surfaces of the arterial wall at physiological pressures to be less than 10%. Stalhand and Klarbring (2005) determined the material and residual strain parameters for a human abdominal aorta (assuming a stress-free configuration of a circular sector) using in vivo pressure–diameter data applied to a Fung type strain energy density function. They also find that the circumferential stress and the circumferential strain are approximately uniform at physiological pressures.

At physiological pressures the radius of the abdominal aorta is approximately 10 mm and the thickness is 1 mm. Neglecting thrombus formation, the ratio of the thickness of the wall to the diameter of the aneurysm will decrease as the aneurysm enlarges, therefore the deformation of the three-dimensional(3D) arterial wall of the developing aneurysm is closely related to the deformation of its midplane. The residual strain that is present in the unloaded configuration gives rise to an approximately uniform strain field through

the thickness of the arterial wall at physiological pressures. If it is assumed that the physiological mechanism by which collagen fibres attach to the artery is independent of both the current configuration of the artery and the radial position in the arterial wall, then the remodelling process may naturally maintain a uniform strain field (in the collagen fibres) through the thickness of the arterial wall as the AAA develops. These considerations thus support the suitability of a membrane model (Wempner 1973; Heil 1996) to model the deformation of the abdominal aorta and development of an aneurysm at physiological pressures.

Watton et al. (2004) model the abdominal aorta as a cylindrical nonlinearly elastic membrane subject to an axial prestretch and a constant internal systolic pressure. The distal and proximal ends of the abdominal aorta are fixed to simulate vascular tethering by the renal and iliac arteries. Formation and development of AAA is assumed to be a consequence of the material constituents of the artery remodelling, whilst subject to a constant systolic pressure. The constitutive relations for the tissue in the model of Watton et al. (2004) incorporate variables that relate to the concentration of the elastin, and to the density and waviness of collagen fibres. This enables the remodelling of the arterial microstructure during AAA development to be addressed. The degradation of elastin is prescribed using a time-dependent axisymmetric function. Collagen fibres are assumed to be in a continuous state of degradation and deposition, and to attach to the artery such that their strain at systole is a constant. As the AAA develops, the deposition and degradation of collagen fibres act to maintain the strain in the fibres within an equilibrium range.

Watton et al. (2004) demonstrated that using a set of physiological material parameters to model the abdominal aorta and realistic remodelling rates for its constituents, the predicted dilations of the aneurysm model were consistent with those observed in vivo. An asymmetric aneurysm with spinal contact is also modelled and the stress distributions are broadly consistent with previous studies. However, the fact that their model of AAA growth achieves realistic dimensions is a factor of its construction. Indeed, the proportion of load initially borne by the collagen, the functional form of the spatial degradation of elastin, the turnover rate of the collagen fibres, the rate at which additional collagen is deposited/lost and the mechanical nonlinearity of the collagen, all directly influence the growth of the aneurysm. In this paper, we examine the effects of varying these influential parameters on the growth rates of the AAA model and compare with clinical observations (Vardulaki et al. 1998; Brady et al. 2004). We also apply a physiological pressure pulse to calculate the steady temporal evolution of the systolic and diastolic geometries of the AAA model. Parameters that characterise the stiffness in terms of the systolic and diastolic configurations can then be determined and compared with physiological studies (Lanne et al. 1992). It is seen that realistic rates of dilation can be achieved for a range of physiologically-consistent geometric, material and remodelling parameters. Moreover, the evolution of the compliance, pressure-strain elastic modulus and stiffness of the AAA model are found to be consistent with published data.

2 Methods

2.1 The recruitment stretch λ_R

As in Watton et al. (2004), we assume that the gross mechanical response of a population of collagen fibrils of varying undulation can be represented by a nonlinear function of stretch, which is defined relative to the onset of recruitment of the fibrils to load bearing. Effectively one can picture an idealised collagen fibre which depicts the mechanical response of a population of collagen fibrils. We assume that the mechanical properties of the idealised fibre remain constant as the tissue remodels, i.e. the undulation distribution of the population of collagen fibrils does not change. This approach allows us to simulate the tissue stress–strain law of a population of fibrils with just a few material parameters.

The stretch in the collagen is defined with respect to the configuration in which it is recruited to load bearing, whilst the stretch in the elastin is always defined with respect to the initial (undeformed) reference configuration. Consider Fig. 1b, which depicts a parallel arrangement of elastin and

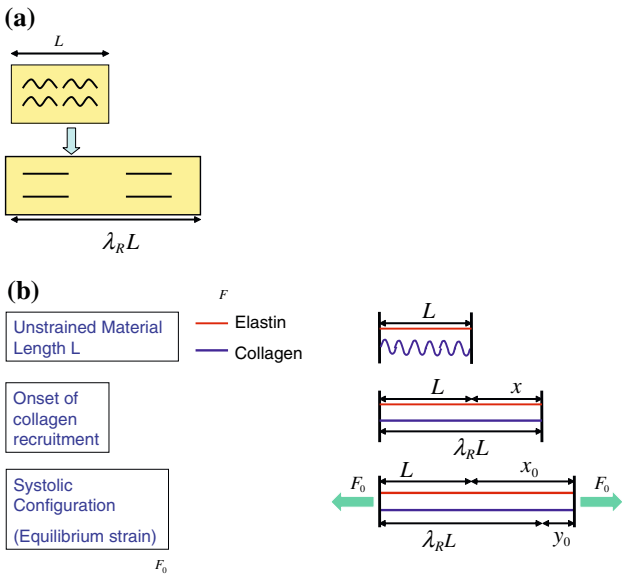

Fig. 1 **a** Collagen fibres are recruited, i.e. begin to bear load, when unstrained tissue is stretched by a factor λ_R. **b** In the unstrained state, the collagen is crimped and the length of elastin is L. A *constant force* is applied to both ends. In equilibrium, the stretch in the collagen is λ_A and thus the G–L strain in the collagen is $E_A = (\lambda_A^2 - 1)/2$

collagen. The length L denotes the length of the unstrained tissue and x its extension. In unstrained tissue, the strain in the elastin is equal to 0, and thus the strain in the elastin is measured with respect to the undeformed configuration. The stretch in the elastin is

$$\lambda = [(L + x)/L]. \tag{1}$$

Collagen fibres are recruited to load bearing when the unstrained tissue is stretched by a factor λ_R. The collagen stretch is defined with respect to the configuration at which it is recruited to load bearing (see Fig. 1), thus

$$\lambda_C = (\lambda_R L + y)/\lambda_R L \tag{2}$$

Now $y = L + x - \lambda_R L$, hence from Eq. (1) and (2) a simple relationship between the elastin stretch and the collagen stretch is obtained:

$$\lambda_C = \frac{\lambda}{\lambda_R} \tag{3}$$

The significance of this relationship, i.e. Eq. (3), is that the recruitment stretch λ_R can remodel to maintain the stretch in the collagen to an equilibrium value whilst the stretch in the elastin increases as the aneurysm dilates. Equivalently: the model adopts distinct reference configurations for the elastinous and collagenous constituents; the reference configuration for the collagenous constituents can adapt.

2.2 The attachment stretch λ_A

An equilibrium stretch λ_A (or *attachment stretch*) for the collagen needs to be defined to enable the remodelling of the collagen to be addressed, as the artery enlarges. The attachment stretch is defined to be the stretch in the collagen (defined with respect to the onset of recruitment to load bearing of a population of collagen fibrils) at systole at $t = 0$. The justification for this definition of λ_A is based on the following hypotheses:

(i) Initially the arterial wall is in a homeostatic state. Although collagen fibrils are in a state of continual deposition and degradation, the gross structural and mechanical properties of the collagen are constant.
(ii) Newly deposited collagen fibrils are acted on by fibroblast cells to attach them to the extra-cellular matrix (ECM) in a state of stretch so that they contribute to the load bearing at physiological pressures. We assume there is a *maximum attachment stretch* that the fibroblasts can achieve.
(iii) we assume that the time taken for the fibroblasts to configure the collagen fibrils is much longer than the duration of a cardiac cycle. This implies that the maximum fibril attachment stretch will occur at the systolic (peak) stretch of the cardiac cycle. Thus the maximum fibril stretch during the cardiac cycle (which will occur at systole) is equal to the maximum attachment stretch.

Fibrils that achieve maximum attachment stretches will have minimum undulation and thus are the first to be recruited to load bearing as the tissue is stretched. If there is a distribution in attachment stretches that the fibroblasts can achieve this would naturally account for the variation in undulation of the fibrils in unloaded tissue. Note also that the definition of a maximum attachment stretch is consistent with the definition of recruitment stretch, which relates to those fibrils (of minimum undulation) which are recruited first to load bearing.

2.3 Collagen remodelling via the recruitment stretch

The remodelling of the recruitment stretch is subtle and it is helpful to visualise what is occurring on the scale of the collagen fibres. Figure 2 portrays the effects of fibre deposition and degradation for a tissue that is stretched and held at fixed length whilst remodelling occurs. Note that the figure depicts *hypothetical collagen fibres*, each of which represents the mechanical response of a population of collagen fibrils of varying undulation. The figure illustrates that the microstructural changes to the tissue, which arise as a result of the physiological turnover of collagen fibres, can be captured by remodelling the recruitment *stretch* λ_R. It is important to appreciate that the time for the tissue to remodel from states (3) to (4) (in Fig. 2) is dependent on the turnover rate of the collagen fibres. Equivalently, the rate at which the recruitment stretch remodels is dependent on the turnover rate of the fibres.

In addition to the recruitment stretches, variables may be introduced which relate to the density of the collagen fibres. This enables the collagen remodelling that occurs during aneurysm development to be modelled.

2.4 Mathematical method

A geometric nonlinear membrane theory (e.g. Wempner 1973; Heil 1996) is adopted to model the deformation of the arterial wall. The abdominal aorta is treated as a thin cylinder of undeformed radius R_0, length L, and thickness H. It is subject to a physiological axial pre-stretch, λ_z^0, and a constant systolic pressure $p_0 (= 16\,\text{kPa} = 120\,\text{mmHg})$ which causes a circumferential stretch of λ_θ^0 he initial in vivo configuration is thus a cylindrical tube of length $\lambda_z^0 L$, radius $\lambda_\theta^0 R_0$, and thickness $H/\lambda_z^0\lambda_\theta^0$.The ends of the initial deformed configuration are spatially fixed to simulate vascular tethering by the renal and iliac arteries. The length of the section of the abdominal aorta between the renal and iliac arteries is taken to be 16 cm which is consistent with physiological values (Raghavan et al. 2006).

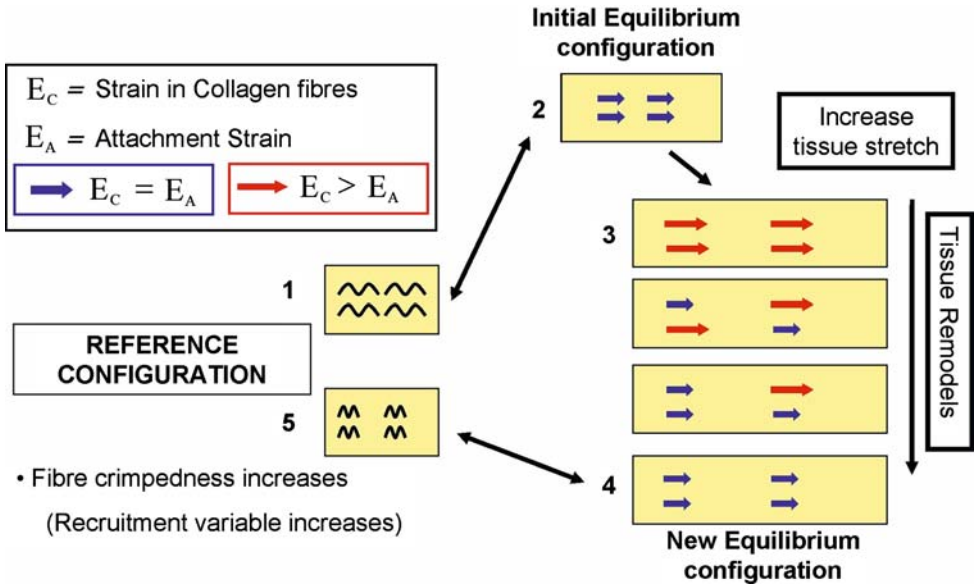

Fig. 2 Attachment of collagen fibres in altered configurations. *1* The reference state is the undeformed configuration of the tissue. In the undeformed state, the fibres have a characteristic waviness. *2* The initial physiological state is such that the strain in the collagen fibres is the equilibrium value, i.e. at systolic pressure the G–L strain in the fibres is E_A. The tissue is currently in equilibrium. Although the fibres are in a continual state of degradation and deposition, new fibres will attach with identical levels of strain to those that decay and thus no changes occur in the mechanical properties of the tissue. *3* Suppose the tissue is stretched further and, for the purposes of this example, held at fixed length. New fibres attach to the tissue so that at the new systolic configuration their G–L strain is E_A. The old fibres decay, and the distribution of collagen fibres changes. The naturally occurring turnover of the fibres will proceed to restore strain in all the fibres to equilibrium levels. *4* All of the old fibres have decayed and have been replaced by new fibres of strain E_A. The artery reaches a new equilibrium configuration. *5* If the tissue is contracted back to the reference configuration, the crimp of the collagen will have increased. Equivalently, the factor the tissue must be stretched for the collagen to be recruited has increased. Hence the effects of deposition and degradation in altered configurations can be captured by remodelling the recruitment stretch λ_R—which relates to the waviness of collagen in the undeformed configuration. Note that the time for the tissue to remodel from state (3) to state (4) is dependent on the turnover rate of the collagen fibres, i.e. the halflife. Equivalently, the rate at which the recruitment stretch remodels is dependent on the turnover rate of the fibres

Details of the mathematical formulation used to model the development of an AAA and numerical implementation can be found in Watton et al. (2004). Here we give an outline of the methodology to avoid unnecessary repetition. The steady deformation of the artery is governed by the principle of virtual displacements,

$$\delta\Pi_{\text{strain}} - \delta\Pi_{\text{load}} = 0, \tag{4}$$

where $\delta\Pi_{\text{strain}}$ represents the variation of the strain energy stored in the arterial wall and $\delta\Pi_{\text{load}}$ is the work done by the pressure during a virtual displacement about an equilibrium displacement field. The variation of the internal elastic energy for a 2D cylindrical membrane is

$$\int_0^{2\pi R}\int_0^{L} \delta(H_{\text{M}}W_{\text{M}} + H_{\text{A}}W_{\text{A}})\mathrm{d}x^1\mathrm{d}x^2, \tag{5}$$

where H_{M} and H_{A} denote the thicknesses of the media and adventitia, respectively, and the integral is evaluated on the midplane of the membrane: $0 \le x_1 \le L$ and $0 \le x_2 < 2\pi R_0$ are the axial and azimuthal Lagrangian midplane coordinates, respectively. The functional forms for the strain–energy density functions (SEDFs) for the media (W_{M}) and adventitia (W_{A}) need to be specified.

2.5 Strain–energy density functions for heterogeneous aneurysmal tissue

The first step in the development of the model is to accurately model the healthy abdominal aorta. The constitutive model proposed by Holzapfel et al. (2000) is utilised. The arterial wall is modelled as two layers. The inner layer models the mechanical response of the media, with contributions from ground substance, elastin and a double helical pitch of collagen fibres. The outer layer models the mechanical response of the adventitia, with mechanical contributions from ground substance and a double helical pitch of collagen fibres. The mechanical response of each layer is modelled as the sum of a neo-Hookean SEDF and a highly nonlinear SEDF which represents the mechanical response of the collagen. Gundiah et al. (2007) confirm the suitability of the neo-Hookean SEDF to represent the mechanical behaviour of elastin. The model of Holzapfel et al. (2000) is adapted to incorporate a degradation function for the elastin, and microstructural recruitment and density variables for the collagen fibres.

We assume that the neo-Hookean response in the media has an elastinous and a non-elastinous part, k_g, due to the ground substance. The elastinous contribution in the media is multiplied by a normalised spatially and temporally dependent concentration of elastin function, $c_E(x_1, x_2, t)$, where $c_E(x_1, x_2, t = 0) = 1$ throughout the membrane. We assume that the contribution from the ground substance is equal in the media and adventitia. The SEDFs are thus

$$W_M = (K_g + c_E(x_1, x_2, t)K_E)(E_{11} + E_{22} + E_{33}) + \sum_{\varepsilon_C^{M_p}, p=\pm} n_{M_p}(x_1,x_2, t) \times K_M\{\exp[A_x(E_C^{M_p}(E_{M_p}, \lambda_R^{M_p}))^2] - 1\} \quad (6)$$

for $x_3 \in [\frac{-H}{2}, \frac{-H+2H_M}{2}]$, and

$$W_A = K_g(E_{11} + E_{22} + E_{33}) + \sum_{\varepsilon_C^{A_p}, p=\pm} n_{A_p}(x_1,x_2, t) \times K_A\{\exp[A_x(E_C^{A_p}(E_{A_p}, \lambda_R^{A_p}))^2] - 1\} \quad (7)$$

for $x_3 \in \left(\frac{H-2H_A}{2}, \frac{H}{2}\right]$. $E_C^{J_p}(x_1, x_2, t)$ denotes the Green–Lagrange (GL) strains in the collagen fibres and $\lambda_R^{J_p}(x_1, x_2, t)$ and $n_{J_p}(x_1, x_2, t)$, are the collagen fibre recruitment and density variables, respectively. J takes values M and A, referring to the media (M) and adventitia (A). The fibres are orientated at angle of γ_{J_p} to the azimuthal axis, where p denotes the pitch $\pm\gamma_J$.

The GL strains of collagen $E_{J_p}^C$ are a function of the GL strains in the elastin resolved in the directions of the collagen fibres, i.e. E_{J_p}, and the recruitment stretches $\lambda_R^{J_p}(x_1, x_2, t)$, where

$$E_{J_p}^C = (E_{J_p} + (1 - (\lambda_R^{J_p})^2)/2)/(\lambda_R^{J_p})^2, \quad (8)$$

and

$$E_{J_p} = E_{11}\sin^2\gamma_{J_p} + E_{22}\cos^2\gamma_{J_p} + 2E_{12}\sin\gamma_{J_p}\cos\gamma_{J_p}, \quad (9)$$

For the axisymmetric model $E_{12} = 0$, thus we can drop the subscript p and denote $E_J \equiv E_{J_+} = E_{J_-}$, i.e. at each point fibres of positive and negative pitch (in both the media and adventitia) have identical values of GL strain. This implies that there are only two independent recruitment variables, i.e. $\lambda_R^J \equiv \lambda_R^{J_+} = \lambda_R^{J_-}$ $(J = M, A)$, and two independent fibre density variables $n_J \equiv n_{J_+} = n_{J_-}$. At $t = 0$, $n_M(x_1, x_2, 0) = n_A(x_1, x_2, 0) = 1$.

The orientations of the collagen fibres in the medial and adventitial layers need to be specified. Holzapfel (2006) determined mean orientations of the medial and advential collagen fibres for an abdominal aorta to be $\pm 37.8°$ and $\pm 58.9°$, respectively. However, whilst the tissue sample exhibited no appreciable disease it was from an elderly specimen (80-year-old female cadaver) and thus the orientations may be unrepresentative values for younger arteries. In fact, fibre orientations are possibly also species and vessel dependent, e.g.: the orientation of collagen fibres in human aortic tissue is $\pm 8.4°$ in the medial layer and $\pm 41.9°$ in the adventitial layer (Holzapfel et al. 2002) whilst fibre orientations in the carotid artery of a rabbit are $\pm 29°$ in the medial layer and $\pm 62°$ in the adventitial layer (Holzapfel et al. 2000). For our model of the human abdominal aorta fibre orientations are chosen to be $\gamma_M = 30°$, $\gamma_A = 60°$.

The thickness of the arterial wall of the abdominal aorta is approximately 2 mm (Mohan and Melvin 1982). Following Holzapfel et al. (2000) we assume the media occupies 2/3 of the thickness of the arterial wall. Note that although that this ratio is based on data for the carotid artery of a rabbit and it is assumed representative of other arteries, e.g. Holzapfel et al. (2000) assumed this to be true for the human left anterior descending coronary artery. We also follow Holzapfel et al. (2000) and assume that the neo-Hookean contribution from the adventitia is an order of magnitude lower than that for the media, i.e. we set $K_g = K_E/10$; this is based on physiological observations for the Youngs modulus of the medial and adventitial layers of porcine thoracic aorta in the reference state (where elastinous constituents dominate mechanical behaviour—see Holzapfel et al. (2000) for discussion) and thus would seem suitable for the abdominal aorta.

The most recent models of the abdominal aorta do not explicitly model the individual contributions from the medial and adventitial layers. Stalhand et al. (2004) determined material and residual strain parameters for a one layered constitutive model (Holzapfel et al. 2000) to fit the in vivo pressure diameter data of Sonneson et al. (1994). Stalhand and Klarbring (2005) adopted a Fung type constitutive model to the same in vivo data and enforced the constraint that the axial force is invariant to the pressure (within the physiological range) to assist parameter determination. Van de Geest et al. (2006) have performed biaxial testing of aneurysmal and non-aneurysmal abdominal aorta however they did not test the medial and adventitial layers independently. Consequently, there is insufficient guidance in the literature to determine the material parameters for the medial and adventitial collagen. In this paper, we have assumed that the ratio of the medial and adventitial collagen material parameters for the carotid artery of a rabbit (Holzapfel et al. 2000) are representative for the human abdominal aorta, i.e. we specify $K_A = K_M/4$. We emphasize this is a purely arbitrary choice: mechanical testing of the individual layers of the abdominal aorta is required to guide the determination of such parameters.

Three independent material parameters, namely K_E, K_M and A_x remain to be determined so that the SEDFs model the mechanical behaviour of the human abdominal aorta.

The pressure–diameter curve of a healthy abdominal aorta is utilised (Lanne et al. 1992) for this purpose. The diastolic and systolic diameters (15 and 17.2 mm) and pressures (80 and 120 mmHg) can be observed directly. However, the experiments were performed in vivo and thus the reference configuration dimensions are unavailable. Hence we take typical physiological values of axial and circumferential stretches from the literature.

Learoyd and Taylor (1966) analysed the retraction of human abdominal aortas and found that older and younger vessels retracted by approximately 30 and 20%, respectively. Consistent with these findings, Holzapfel et al. (2007) found the average in situ axial stretch of seven human abdominal aortas to be 1.19 ± 0.084. We choose $\lambda_z^0 = 1.3$—which represents an upper bound for the axial pre-stretch of the human abdominal aorta. Langewouters et al. (1984) analysed the static elastic properties of 20 abdominal aortas in vitro: from their data the average circumferential stretch of 11 abdominal aortas from patients of ages ranging from 30 to 59 can be determined to be 1.29. This is consistent with the findings of Stalhand and Klarbring (2005) who used an axial force constraint to identity in vivo parameters of the abdominal aorta—they predicted a circumferental stretch of 1.27 at a systolic pressure of 16 kPa.

Assuming a circumferential stretch of 1.3 and utilising the pressure–diameter data of Lanne et al. (1992), i.e. systolic diameter of 17.2 mm, this implies a diameter of approximately 13.2 mm in the reference configuration. We assume that the onset of collagen recruitment occurs between the diastolic and systolic diameters (Armentano et al. 1995), and arbitrarily estimate this to occur at a diameter close to the diastolic diameter, i.e. 15.2 mm. Initial values for the recruitment variables are then calculated to be $\lambda_{\mathrm{R}}^{\mathrm{M}}(t=0) = 1.19$, $\lambda_{\mathrm{R}}^{\mathrm{A}}(t=0) = 1.19$ and the equilibrium attachment G–L strain is $E_{\mathrm{A}} = (\lambda_{\mathrm{A}}^2 - 1)/2 = 0.098$.

To determine the three unknown material parameters K_{E}, K_{M} and A_x we analyse the governing force-balance equation for a cylindrical membrane of fixed axial stretch subject to radial inflation:

$$p = \left\{ \frac{1}{R_0\lambda_z}\left[(H_{\mathrm{M}} + H_{\mathrm{A}})K_{\mathrm{g}} + H_{\mathrm{M}}c_{\mathrm{E}}K_{\mathrm{E}}\left(1 - \frac{1}{\lambda_z^2\lambda_\theta^4}\right)\right]\right\} + \left\{ \frac{1}{R_0\lambda_z} \sum_{J=\mathrm{M,A};\varepsilon_J^C \geq 0} \frac{4n_J H_J K_J A_x E_J^C \exp[A_x (E_J^C)^2]\cos^2\gamma_J}{(\lambda_{\mathrm{R}}^J)^2} \right\} \tag{10}$$

where the first- and second-terms on the right-hand side of Eq. (10) correspond to the contribution to load bearing from the elastinous and collagenous constituents, respectively. Equation (10) is derived from the governing varational equation [i.e. Eq. (4)], the functional form of the strain energy density functions (Eqs. 6, 7) and consideration of the displacement field for a cylindrical membrane. Full details of the derivation can be found in Watton et al. (2004).

Now for an artery subject to a fixed axial pre-stretch and subject to radial inflation, Eq. (10) can be written more succinctly as

$$\begin{aligned} p(\lambda_\theta) &= P_{\mathrm{E:C}}\, p(\lambda_\theta) + (1 - P_{\mathrm{E:C}})\, p(\lambda_\theta) \\ &= f_{\mathrm{E}}(K_{\mathrm{E}}, \lambda_\theta) + f_{\mathrm{C}}(K_{\mathrm{C}}, A_x, \lambda_\theta) \end{aligned} \tag{11}$$

where $P_{\mathrm{E:C}}$ denotes the proportion of load borne by the elastinous constituents at $t = 0$; and thus $(1 - P_{\mathrm{E:C}})$ represents the proportion of load borne by the collagen at $t = 0$. The functions $f_{\mathrm{E}}(K_{\mathrm{E}}, \lambda_\theta)$ and $f_{\mathrm{C}}(K_{\mathrm{C}}, A_x, \lambda_\theta)$ represent the mechanical contribution to load bearing from the elastin and collagen, respectively; they can be explicitly identified from the first-and second-terms on the right-hand side of Eq. 10. Given a value for $P_{\mathrm{E:C}}$ at systolic pressure ($p = p_0$), this enables K_{E} to be determined immediately:

$$P_{\mathrm{E:C}}\, p_0 = f_{\mathrm{E}}(\lambda_\theta^0, K_{\mathrm{E}}) \Rightarrow K_{\mathrm{E}} = f_{\mathrm{E}}^{-1}(P_{\mathrm{E:C}}\, p_0, \lambda_\theta^0). \tag{12}$$

An additional equation is required to determine the remaining material parameters, K_{M} and A_x. We consider the diameter at a second, greater pressure ($p = p_{200} = 200$ mmHg, $\lambda_\theta = \lambda_\theta^{200}$). This yields two equations,

$$\begin{aligned} (1 - P_{\mathrm{E:C}})\, p_0 &= f_{\mathrm{C}}(K_{\mathrm{C}}, A_X, \lambda_\theta^0), \\ p_{200} &= f_{\mathrm{E}}(\lambda_\theta^{p=200}) + f_{\mathrm{C}}(K_{\mathrm{C}}, A_{X,} \lambda_\theta^{p=200}) \end{aligned} \tag{13}$$

thus enabling the two remaining constants, K_{M} and A_{x}, to be determined.

A value for the parameters $P_{\mathrm{E:C}}$ needs to be specified. Armentano et al. (1995) proposed a simple 1-D model to account for the individual mechanical contributions to load bearing of the elastinous and collagenous constituents for the aorta of a conscious dog. Their model predicts that at systolic pressure, the elastin bears 88% of the load, i.e. $P_{\mathrm{E:C}} \approx 0.9$ for an aorta. Given that human arteries naturally lose elasticity as they age (Lanne et al. 1992; Wuyts et al. 1995), this suggests that 0.9 is a suitable upper bound for $P_{\mathrm{E:C}}$. For the default model of the abdominal aorta, we assume a slightly lower value, i.e. $P_{\mathrm{E:C}} = 0.8$. However, lower values of $P_{\mathrm{E:C}}$ may be more appropriate given that AAA generally occurs in older individuals. Therefore we consider the influence of this parameter on growth of the AAA model for $0.1 \leq P_{\mathrm{E:C}} \leq 0.9$.

Figure 3 illustrates a pressure–diameter relationship for our model of the abdominal aorta and illustrates the individual contributions to load bearing of the elastin and the collagen. Note, the material parameters summarised in Table 1 (and correspondingly the pressure–diameter relationship depicted in Fig. 3) are based on $P_{\mathrm{E:C}}(\lambda_\theta = \lambda_\theta^0) = 0.8$. Note that for our model of the abdominal aorta, the systolic (diastolic) axial and azimuthal Cauchy stresses are 102.9 kPa (87.4 kPa) and 116.5 kPa (78.3 kPa), respectively. The axial force is 3.97 N at diastole and 3.34 N at systole.

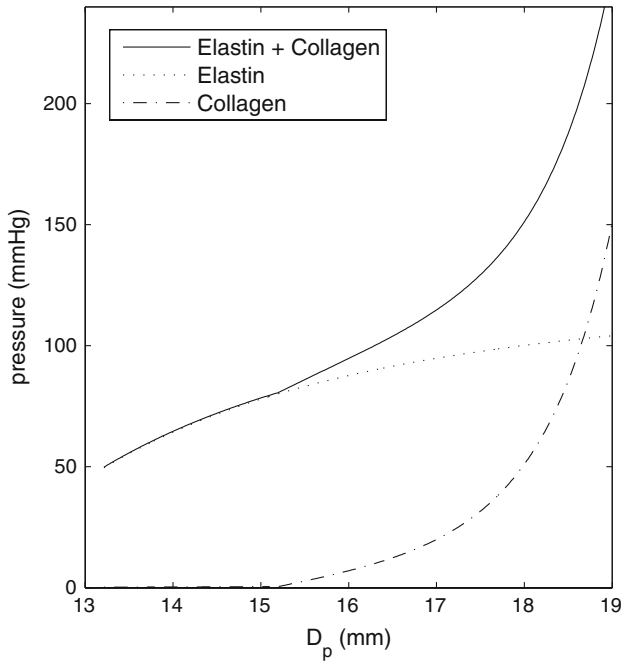

Fig. 3 Pressure–diameter relationship for the model of the abdominal aorta. The diameter of the abdominal aorta in the reference configuration is taken to be 13.2 mm. The diastolic and systolic diameters are $D_{\mathrm{DIAS}} = 15$ mm and $D_{\mathrm{SYS}} = 17.2$ mm, respectively. Recruitment of collagen to load bearing is estimated to begin at $D_{\mathrm{DIAS}} = 15.2$ mm. Collagen bears one-fifth of the load at systole

Table 1 Material constants and physiological data used for modelling the human abdominal aorta

Wall thickness:		
Media	H_{M}	1.33 mm
Adventitia	H_{A}	0.67 mm
Fibre orientation		
Media	γ_{M}	30°
Adventitia	γ_{A}	60°
Systolic pressure	p_0	120 mmHg
Undeformed radius	R_0	6.6 mm
Axial pre-stretch	λ_z^0	1.3
Circumferential stretch:		
At onset of recruitment	$\lambda_\theta^{\mathrm{rec}}$	15.2/13.2
At Systole	λ_θ^0	17.2/13.2
At $p = p_{200} = 200$ mmHg	λ_θ^{200}	18.5/13.2
Material Parameters:		
Elastin	K_{E}	97.6 kPa
Ground substance	$K_{\mathrm{g}} = K_{\mathrm{E}}/10$	9.76 kPa
Collagen media	K_{M}	3.52 kPa
Collagen adventitia	$K_{\mathrm{A}} = K_{\mathrm{M}}/4$	0.88 kPa
Exponential constant for collagen	A_x	40

This data is estimated using the pressure–radius curve for the abdominal aorta in (Lanne et al. 1992) and physiological measurements of axial (Learoyd and Taylor 1966) and circumferential stretches (Langewouters et al. 1984) at systole

2.6 Elastin degradation

The dilation of an AAA is accompanied by loss of elastin (He and Roach 1993; Shimizu et al. 2006). The half-life of elastin is approximately 50 years, consequently the loss of elastin in adults almost certainly results from increased elastolysis rather than insufficient synthesis (Shimizu et al. 2006). However, the physiological processes that lead to the degradation of elastin in AAA are not clearly understood. One suggestion is that the degradation may be linked to the uptake of oxidised cholesterol through the arterial wall (Davies 1998). This suggests a progressive degradation of elastin over time. However, the functional form of the spatial degradation is unknown. We assume that there is a point in the central region of the domain where elastin degradation begins, and in the developed aneurysm this region has been degraded the most. This functional form should give rise to a fusiform dilatation of the abdominal aorta centred in the computational domain. One such suitable candidate for the degradation function is

$$c_{\mathrm{E}}(x_1, t) = 1 - (1 - (C_{\min})^{t/T}) \exp[-\mu(1 - 2x_1/L)^2], \tag{14}$$

where L denotes the axial Lagrangian length of the membrane, $\mu \geq 0$ controls the width of the degradation, and $C_{\min}$ is the minimum concentration of elastin at time $t = T$. Specifying $\mu = 0$ yields a uniform degradation throughout the domain. Increasing the value of μ increases the spatial localisation of the degradation about a point of minimum concentration in the centre of the axial domain.

The timescale of aneurysm development may vary from person to person. Given that average growth rate is 0.4 cm/year (Humphrey 2002), and the decision whether to operate on an aneurysm occurs when the diameter reaches 5.5 cm, then the timescale of development is of the order of 10 years. Estimates suggest that 63–92% of the elastin is lost in aneurysmal tissue (He and Roach 1993), i.e. $0.08 \leq C_{\min} \leq 0.37$. Consequently, we choose default values for these parameters within this range, specifically $C_{\min}$=0.2, T=10.

The localisation of degradation of elastin is varied by considering a range of values for the parameter μ, namely $0 \leq \mu \leq 160$, and the resulting axial profiles of developed aneurysms are analysed. (It is observed that $\mu = 20$ yields satisfactory results — see Section 3)

2.7 Collagen remodelling

The turnover of collagen is simulated by proposing remodelling equations that act to maintain the G-L strain in the collagen fibres to an equilibrium value E_{A} (equivalently remodelling the stretch of the collagen fibres to λ_{A}). This is achieved by remodelling the reference configuration of the collagen fibres, i.e. remodelling the recruitment stretches. In

addition, it is assumed that changes in the density of the collagen fibres are driven by deviations of the collagen strain from equilibrium values.

For the axisymmetic model, two independent recruitment variables and two independent fibre density variables are required. In the absence of physiological data, linear differential equations are proposed for the remodelling of the recruitment and density variables, i.e.

$$\frac{\partial \lambda_{\mathrm{R}}^{J}}{\partial t} = \alpha(E_J^{\mathrm{C}} - E_{\mathrm{A}}), \quad \frac{\partial n_J}{\partial t} = \beta(E_J^{\mathrm{C}} - E_{\mathrm{A}}), \tag{15}$$

where $\alpha, \beta > 0$ and $E_{\mathrm{A}} = (\lambda_{\mathrm{A}}^2 - 1)/2$. The remodelling parameter α can be determined numerically so that it corresponds to a prescribed half-life, α_{H} (months), of the collagen fibres, i.e. $\alpha = \alpha(\alpha_{\mathrm{H}})$ (Watton 2002). Given that collagen in the arterial wall typically has a half-life of 60 days, we assume a default value of $\alpha_{\mathrm{H}} = 2$. However, turnover rates may increase (Nissen et al. 1978) or decrease (Carmo et al. 2002) in pathological conditions. Consequently we explore a range of collagen half-lives, viz. $0.1 \leq \alpha_{\mathrm{H}} \leq 6$, to explore the influence of this physiological parameter on AAA growth.

The growth rate parameter β relates to the rate at which additional collagen is deposited and configured within the arterial wall. It is numerically determined so that the dilation is physiologically consistent over a timescale typical of aneurysm development: we assume that the diameter increases by a factor of 2–3 over a period of 10 years.

Note there is a distinction between *growth* and *remodelling*. Here the recruitment variables capture the *remodelling* of the tissue, i.e. the gross microstructural changes that occur within the tissue due to the natural physiological process of fibre deposition and degradation, in altered configurations, for a fixed mass of collagen constituents. The collagen density variables relate to the *growth/atrophy* of the collagenous constituents within the arterial wall.

2.8 Analysis of mechanical properties of the AAA model

To analyse the evolution of clinically measurable mechanical parameters, the diastolic deformations are calculated as the aneurysm evolves. At each time step of the computational simulation, the pressure is incrementally decreased from systolic to diastolic values to calculate the geometry of the AAA at all pressures. A clinical measure (Lanne et al. 1992) of the strain in the AAA wall, ε, is calculated, i.e.

$$\varepsilon = \frac{D_p - D_{\mathrm{dias}}}{D_{\mathrm{dias}}} \tag{16}$$

where D_p is the maximum diameter at a pressure p, and D_{dias} the maximum diameter of the AAA at diastolic pressure. The maximum fractional diameter change, $\varepsilon_{\max}$, or maximum arterial strain (Lanne et al. 1992) is thus $\varepsilon_{\max} = \varepsilon|_{D_p = D_{sys}}$, where D_{sys} is the maximum diameter at systole.

The pressure–strain elastic modulus, E_p, is given by

$$E_p = k\frac{P_{\mathrm{sys}} - P_{\mathrm{dias}}}{(D_{\mathrm{sys}} - D_{\mathrm{dias}})/D_{\mathrm{dias}}}, \tag{17}$$

where $k = 133.3$ is a conversion parameter so that E_p is measured in N/m^2. P_{sys} (=120 mmHg) and P_{dias} (=80 mmHg) are the systolic and diastolic blood pressure. Due to the nonlinear pressure–diameter relationship of the arterial wall, E_p is pressure dependent. A stiffness parameter, γ, that appears to characterise the entire deformation of the arterial wall without pressure dependence (Lanne et al. 1992) is

$$\gamma = \frac{\ln(P_{\mathrm{sys}}/P_{\mathrm{dias}})}{(D_{\mathrm{sys}} - D_{\mathrm{dias}})/D_{\mathrm{dias}}}. \tag{18}$$

Note, higher values of E_p and γ imply that the artery is stiffer and less distensible and thus has a lower compliance.

2.9 Overview of the model

To summarise the model: Eqs. (6) and (7) are the (spatially and temporally) heterogeneous SEDFs of the medial and adventitial layers of the arterial wall, which account for independent reference configurations for the elastin and collagen at each point in the tissue. Equation (14) represents the concentration of elastin which degrades in a spatially prescribed manner over time. Equation (15) (left) acts to maintain the GL strain in the collagen to E_{A} by remodelling the reference configuration of the collagen fibres, i.e. it simulates the consequence of fibre deposition and degradation in altered configurations. The second of equations (15) controls the remodelling of the collagen fibre density. Equation (4) governs the equilibrium displacement field and is solved by a finite element method coded in FORTRAN 77.

3 Results

3.1 Axisymmetric AAA growth

We illustrate the development of an AAA that arises due to an axisymmetric degradation of elastin. The default set of parameters we use for the AAA growth model to achieve realistic dilation are:$\alpha_H = 2$, $\beta = 25$, $C_{\min} = 0.2$, $\mu = 20$, $P_{\mathrm{E:C}} = 0.8$. [1] Figure 4a shows the concentration of elastin (as a function of the Lagrangian coordinate,$x_1' \in [0, L]$, see Eq. 23) and Fig. 4b its evolving geometry every 2 years. The grid in the illustration (Fig. 4b) enables deformation of material points on the arterial wall to be visualised: notice the

[1] Note that in Watton et al. (2004) the stated half-life used was 6 months, however a numerical mistake in the computational code actually meant that the half-life used was 0.6 months. This should be borne in mind when comparing their results with this paper.

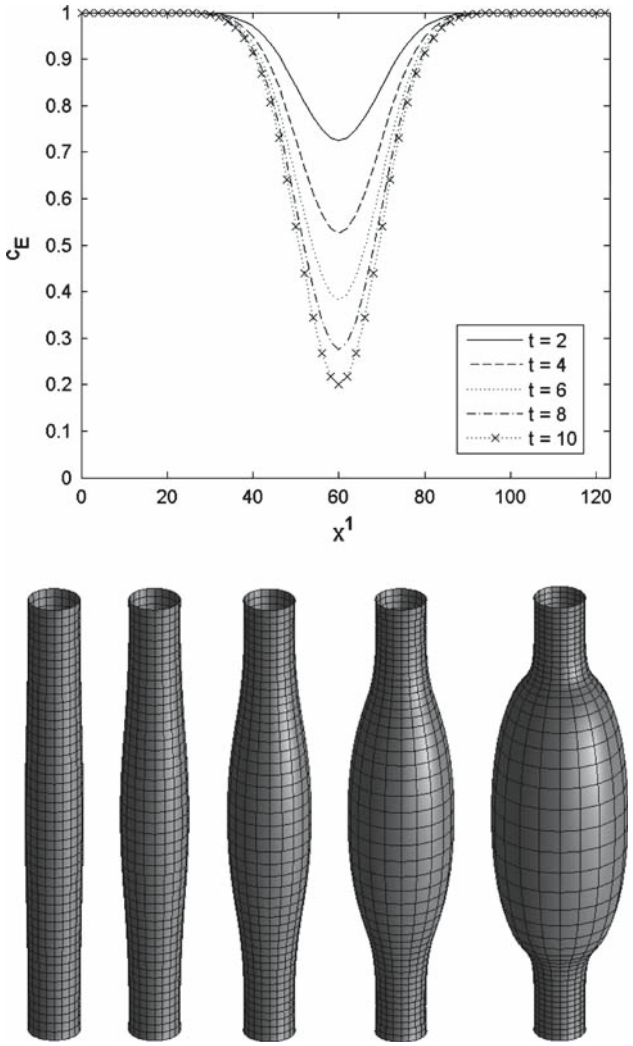

Fig. 4 **a** Prescribed concentration of elastin as a function of the Lagrangian coordinate x_1 (see Eq. 23) using $\mu = 20$, $C_{\min} = 0.2$, $L = 160/\lambda_z^0$, $T = 10$, $x_1^i \in [0, L]$ (Note: no circumferential variation). **b** A developing axisymmetric aneurysm, $t = 2, 4, 6, 8, 10$ years from *left* to *right*. Notice the axial dilation of the central region of the aneurysm and retraction of the ends. Remodelling parameters are $\alpha_H = 2$, i.e. a half-life of 2 months, and $\beta = 25$. The grid is for visualisation only and indicates the relative deformation of points on the arterial wall

model predicts that AAA growth is accompanied by an axial dilation of the central region of the artery and a retraction of its distal and proximal ends.

However, the fact that our model of AAA development achieves physiological dimensions (Fig. 4b) can partly be attributed to its construction and selection of parameters. Indeed, there exists a set of pairs of remodelling parameters, (α_H, β) which can be numerically determined to achieve identical systolic diameters at $t = 10$. Assuming a physiological range for the collagen half-life, i.e. 0.1–3 months, the following remodelling parameter pairs, $(\alpha_H, \beta) = (0.1, 950)$, $(0.5, 195)$, $(2, 25)$, $(3, 10)$ and $(6, 0)$ all yield a systolic diameter of approximately 45 mm at $t = 10$ (see Fig. 5a). We include the case $\alpha_H = 6$ in this analysis as this achieves a realistic dilation with no remodelling of the fibre density, and thus represents an upper bound for the collagen half-life predicted by our mathematical model. Figures 5b and c illustrate the rate of growth as a function of the systolic diameter and time, respectively. It is seen that as the half-life is decreased to achieve realistic dilation at $t = 10$, the growth rate progressively decreases at earlier times and is more rapid at later times. Interestingly, in all cases considered here the rate of growth evolves approximately linearly with respect to the diameter (Fig. 5c). For an AAA of diameter 45 mm, the predicted growth rates range from 4 to 26 mm/year for $\alpha_H = 6$ to $\alpha_H = 0.1$, respectively.

Next, consider the evolution of the diameter as the remodelling parameters α_H and β are varied independently. First α_H is varied whilst $\beta = 0$, i.e. there is no increase in collagen content within the wall as the AAA develops. Increasing the turnover rate of the fibres, i.e. decreasing α_H, increases the rate of dilation and increases the nonlinearity of the dilation (see Fig. 6a). Figure 6b illustrates evolving systolic diameters for $\alpha_H = 2$ and $\beta = \{0, 5, 15, 25, 50, 100\}$. It can be seen that increasing the rate at which the artery can deposit new collagen, i.e. increasing the value of β, reduces the rate of dilation.

To illustrate the dependency of growth on the elastin degradation function (Eq. 23), the parameter μ is varied from $\mu = 0$ (the special case of uniform degradation throughout the domain) to $\mu = 320$ a very localised degradation in a central region of the domain: Fig. 7a shows the degradation (as a function of the Lagrangian coordinate) at $t = 10$ for 7 cases ($\mu = 0,\ 0.25,\ 0.5,\ 15,\ 20,\ 80,\ 320$) and Fig. 7c the corresponding axial geometries. It is observed: for $\mu \leq 1$ the geometry of the AAA is constrained by the fixed boundary conditions at the end of the domain; for $5 \leq \mu \leq 80$, aneurysms of similar diameters develop and the geometry of the AAA does not appear to depend on the fixed radial position of the boundaries (but it still depends on the axial position of the boundaries); for $\mu \geq 160$, the aneurysms become progressively smaller. It can be seen that $5 \leq \mu \leq 80$ yields aneurysms of maximum diameters in the range 42–44 mm that display a characteristic bulge in the central region of the domain. For our default model, we choose $\mu = 20$, this yields an appreciable bulge which is not unduly influenced by the boundary conditions at the ends of the domain.

The parameter $P_{\text{E:C}}$ defines the proportion of load initially borne by the elastin at systolic pressure. The influence of this parameter on the evolving diameter of the AAA is shown in Fig. 8. As to be expected, increasing $P_{\text{E:C}}$ renders the artery more sensitive to the degradation of elastin and faster rates of dilation are observed; the converse of this is clearly true.

Lastly we consider the effect of varying the parameter A_x, which governs the mechanical nonlinearity of the colla-

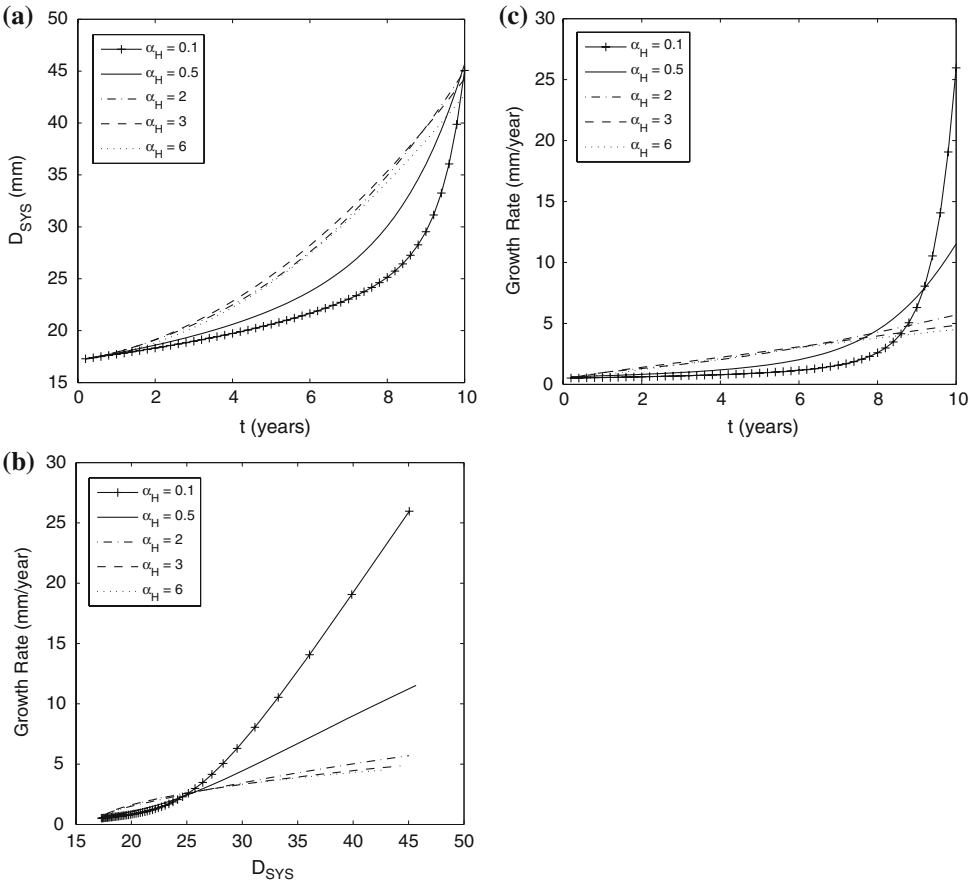

Fig. 5 Various combinations of α_H, β can be chosen to yield an aneurysm of physiological dimensions at t = 10, e.g. $(\alpha_H, \beta) = (0.1, 950)$, (0.5, 195), (2, 25), (3, 10) and (6, 0). Evolution of **a** the systolic diameter D_{SYS} and **b** growth rate with respect to time. It is observed that half-lives of 2–6 months yield a steady evolution of the diameter. As the half-life is reduced further, to achieve a physiological dilation at $t = 10$ the model predicts growth with increasing non-linearity. **c** Evolution of the growth rate as a function of the systolic diameter D_{SYS}. The rate of growth increases linearly ($D_{SYS} > 25$ mm) with respect to the diameter in all cases—this observation suggests that the diameter of the aneurysm increases exponentially with respect to time for this model of AAA

gen, on AAA growth. Figure 9a shows the pressure–diameter relationships for an artery held at fixed axial pre-stretch and maintaining a cylindrical geometry as the pressure is increased for a range of values: $A_x = 10,\ 20,\ 40,\ 80, 160$. Note that (i) $A_x = 40$ is the default physiological case determined from the data of Lanne et al. (1992); (ii) in all cases, the proportion of the load borne by elastin at systole is 0.8, i.e. $P_{E:C} = 0.8$; and (iii) increasing A_x increases the mechanical nonlinearity of collagen and the arterial wall. Figure 9b shows the evolution of the diameter with time for each value of A_x considered. It can be seen that the greater the stiffness of the collagen, the lower the rate of dilation.

3.2 Evolution of the mechanical properties of the AAA model

The default aneurysm model [see Figs. 4 and 6 for the case $(\alpha_H, \beta) = (2, 25)$] is subjected to a physiological pressure pulse (Fig. 10a) as it develops. Figure 10b illustrates the strain in the aneurysm wall (see Eq. 25) as the pressure is increased from diastolic (80 mmHg) to systolic (120 mmHg). The ten curves represent the pressure-strain behaviour of the aneurysm for each year of development. It can be seen that the curves become progressively steeper for each subsequent year, and that for any given value of pressure, the stiffness increases as the aneurysm increases in size, i.e. the gradient of the pressure–strain curves progressively increases.

The evolution of ε_{max}, E_p and γ with respect to time are illustrated in Fig. 11a–c for the five remodelling parameter sets illustrated in Fig. 5, i.e. $(\alpha_H, \beta) = (0.1, 950)$, (0.5, 195), (2, 25), (3, 10) and (6, 0). In all cases considered, ε_{max} decreases from 0.13 to approximately 0.02. E_p and γ increase from 0.4×10^5 N/m^2 and 3 to $1.7 \leq E_p \leq 3 \times 10^5$ N/m^2 and $16 \leq \gamma \leq 30$, respectively. If ε_{max}, E_p and γ are plotted against the maximum diameter (Fig. 11d–f), it can be seen that ε_{max} falls in an exponential manner, and that the rates of increase of E_p and γ decrease as the diameter enlarges.

4 Discussion

Our analysis suggests that the more compliant the artery, in particular increased values of $P_{E:C}$ and/or decreased values of A_x, produce faster AAA dilation rates (Figs. 8, 9). Given that arteries naturally increase in stiffness with age, this would suggest that the growth rates of AAA may depend on the patient's age. However, if younger arteries have a better adaptive response, and thus can respond more rapidly to

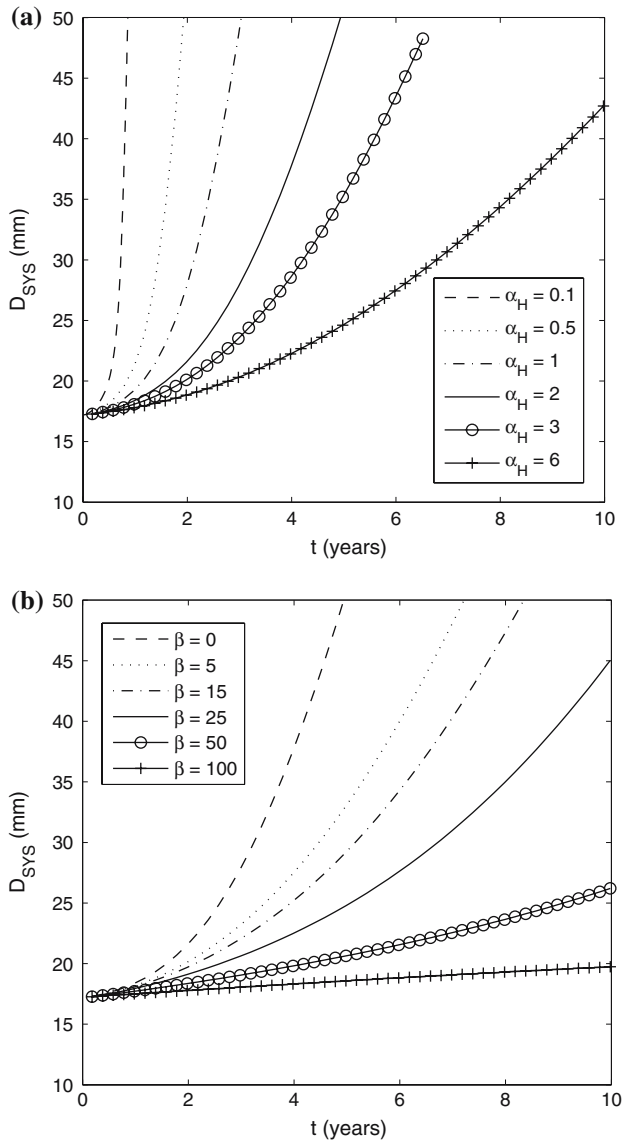

Fig. 6 **a** Dilation of the aneurysm with a range of collagen half-lives, i.e. $\alpha_H = \{0.1,\ 0.5, 1,\ 2,\ 3,\ 6\}$ and prescribing no remodelling of the collagen density, i.e. $\beta = 0$. Dilation rates increase as the collagen half-life is decreased. **b** Dilation of the aneurysm for a half-life of 2 months, i.e. $\alpha_H = 2$, with $\beta = \{0,\ 5,\ 15,\ 25,\ 50,\ 100\}$. Increasing the value of β increases the rate of collagen deposition and thus decreases the rate of aneurysm growth

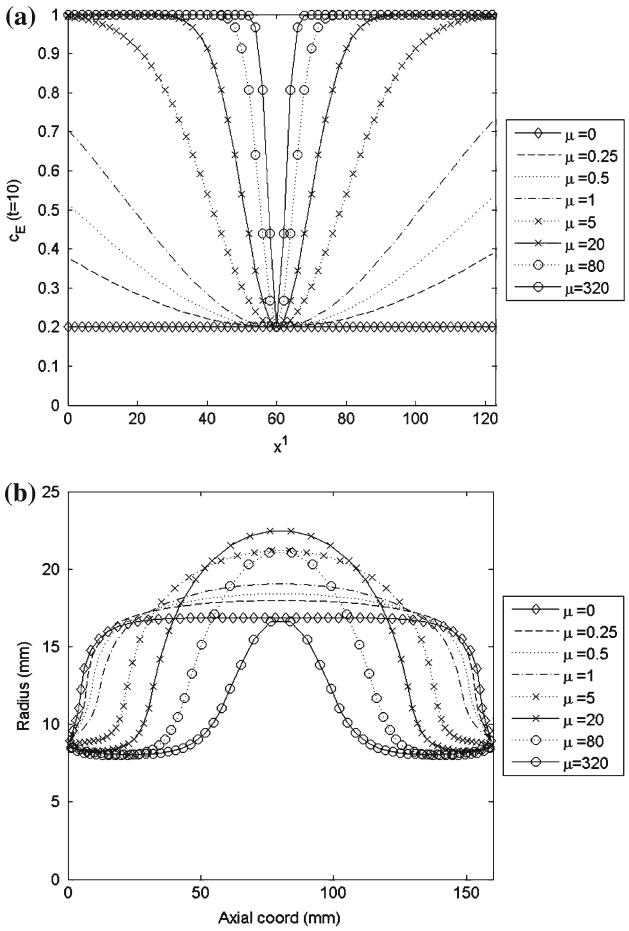

Fig. 7 **a** Different functional forms for the degradation function obtained by varying the parameter μ (see Eq. 23). The axisymmetric degradation varies from being spatially uniform ($\mu = 0$) to highly localised in the centre of the domain ($\mu = 320$). **b** Axial profiles of developed aneurysms at $t = 10$ years for various degrees of spatial degradation of the elastin. It is observed that: for $\mu \leq 1$ the geometry of the aneurysm is constrained by the fixed boundary conditions at the end of the domain; for $5 \leq \mu \leq 80$ aneurysms of similar diameters develop and the geometry of the aneurysm is not dependent on the fixed boundary conditions; and for $\mu \geq 160$, the aneurysms become progressively smaller. In this work we choose $\mu = 20$, this achieves an appreciable bulge which is not unduly influenced by the boundary conditions at the ends of the domain

deposit new collagen, differences in dilation rates may not be observed.

Interestingly, we find an approximate linear relationship between the *growth rate* and the diameter of the aneurysm (see Fig. 5c) for all five sets of remodelling parameters considered, i.e. $(\alpha_H, \beta) = (0.1, 950)$, $(0.5, 195)$, $(2, 25)$, $(3, 10)$ and $(6, 0)$. Thus the model predicts that the diameter $d(t)$ of an AAA increases exponentially over time, i.e.

$$\frac{\mathrm{d}[\mathrm{d}(t)]}{\mathrm{d}t} = C\mathrm{d}(t) \Rightarrow \mathrm{d}(t) = A\exp(Ct) \quad A, C > 0. \tag{19}$$

The prediction that the rate of growth increases as the aneurysm enlarges is consistent with clinical observations, e.g. Vardulaki et al. (1998) and Brady et al. (2004). Indeed, Vardulaki et al. (1998) applied an exponential growth model to determine a mean average growth rate from clinical data. They found that AAAs of diameters in the ranges, 30–39 mm, 40–49 mm and 50 mm+ increased in diameter by 0.69, 1.5 and 3.2 mm/year, respectively. However, Brady et al. (2004) concluded that a quadratic growth law is more suitable: average growth rates of AAAs with diameters ranging from 28–39 mm, 40–45 to 46–85 mm were 1.85, 2.69 and 3.5 mm/year, respectively.

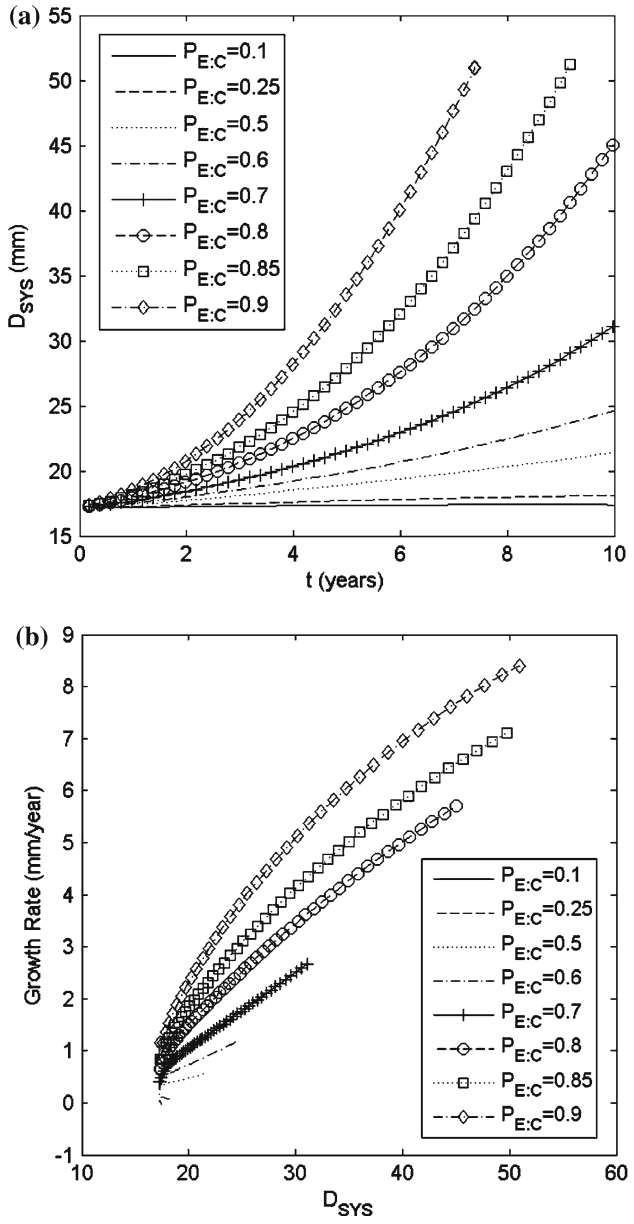

Fig. 8 The evolution of the systolic diameter as a function of time for varying initial values of $P_{\mathrm{E:C}}$; the parameter that governs the relative load borne by the elastinous constituents of the arterial wall, at systolic pressure, at the start of the simulation, i.e. $t = 0$. Increasing $P_{\mathrm{E:C}}$, results in an increased (mechanical) sensitivity of the arterial wall to elastin degradation, with the consequence that the rate of dilation increases

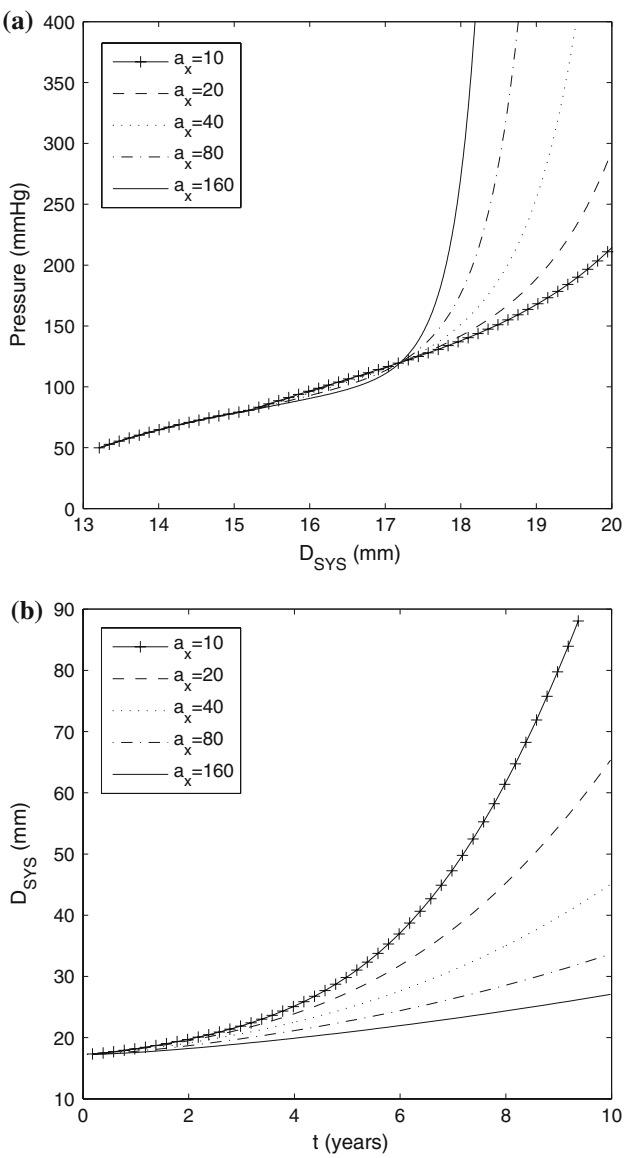

Fig. 9 **a** Pressure–diameter relationship for varying values of the collagen exponential stiffness parameter A_x. Note that the default value is $A_x = 40$ (estimated using data from Lanne et al. 1992). In all cases, at the systolic pressure (120 mmHg), the diameter of the healthy artery is 17.2 mm and the collagen bears 1/5 of the load, i.e. $P_{\mathrm{E:C}} = 0.8$. Increasing A_x increases the mechanical nonlinearity of the collagen (and the artery). **b** The evolution of the diameter as a function of time for $10 \leq A_x \leq 160$. Increasing the value of A_x increases the nonlinear mechanical response of the collagen fibres (a) and the effect of this is to reduces the rate of growth of the diameter of the aneurysm

On inspection of Fig. 5b it can be seen that using a half-life of the collagen of 2 months, i.e. $\alpha_H = 2$, our model predicts that AAAs of diameters 25, 35 and 45 mm have growth rates of approximately 2.6, 4.3 and 5.7 mm/year, respectively. Longer half-lives produce slower rates of dilation. Interestingly, a collagen half-life of 6 months just achieves realistic dilation rates after 10 years with no remodelling of the fibre density, i.e. $\alpha_H = 6$ is an upper bound for our growth model of the AAA. Shorter half-lives, i.e. $\alpha_H \leq 0.5$, produce unrealistically high rates of dilation: half-lives of 0.5 and 0.1 months yield maximum growth rates of 12 and 26 mm/year, respectively. This may suggest that half-lives of the order of months are the most suitable for modelling steady AAA development. This is consistent with the experimental observation by Nissen et al. (1978) that collagen of the normotensive rat aorta has a typical half-life of 60–70 days. However, it is

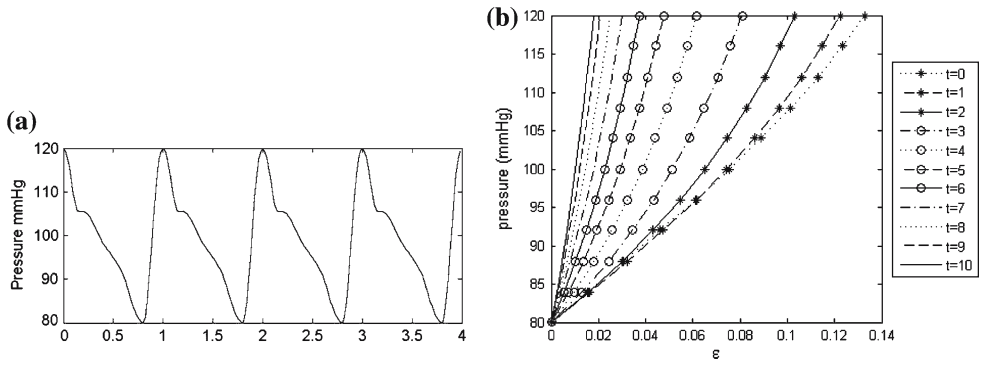

Fig. 10 **a** Physiological pressure pulse is applied to the AAA model. **b** The arterial diameter strain, ε, as a function of the pressure. Each of the 11 curves corresponds to the pressure–strain behaviour at yearly time intervals. The gradient of each curve increases as the pressure increases, i.e. the aneurysm becomes stiffer as it increases in size. Also, for any given pressure, the stiffness of the aneurysm increases with time. Note, this example uses the default set of parameters: $\mu = 20$, $P_{\mathrm{E:C}} = 0.8$, $A_x = 40$, $\alpha_H = 2$, $\beta = 25$

unclear how turnover rates of fibres will change as the aneurysm progresses. Carmo et al. (2002) report an increase in collagen cross-links in aneurysm aortic walls and suggest the synthesis of new collagen could be stopped whilst existing collagen continues to accumulate cross-links, i.e. reduced turnover rates. However, in the hypertensive aorta and mesenteric arteries of a rat turnover rates reduce to 17 days in hypertensive conditions. It may be that a sudden increase in enzymatic activity that is not balanced by increased matrix deposition is the predisposing factor for rupture. Given the rapidity of tissue remodelling, this could be a relatively quick event.

The fact that AAAs of realistic dimensions can be developed is partly a factor of the construction of our model. We have illustrated that growth is sensitive to several key parameters in the model, e.g. the half-life of the collagen fibres, α_H (Fig. 6a), the growth rate parameter β (Fig. 6b), the elastin degradation function (Fig. 7c), the proportion of load initially borne by the collagen, $P_{\mathrm{E:C}}$ (see Fig. 8a), and the mechanical nonlinearity of the collagen A_x (Fig. 9b). Thus given the uncertainty in these parameters, the model as it stands cannot be used to predict growth rates on a patient-specific basis. However, there would appear to be potential for the values of these parameters to be more accurately known: the parameters $P_{\mathrm{E:C}}$ and A_x are both parameters that could be estimated from physiological data to yield a structural model of the abdominal aorta as it ages; accurate functional representations for the degradation of elastin could be determined; the half-life collagen fibres, α_H, in aneurysmal tissue could be determined, and then a suitable value for β could be prescribed from knowledge of the current diameter and growth rate of an individuals AAA.

The AAA model can produce a range of realistic dilation and growth rates for a physiological range of input parameters. However, it has been demonstrated that there is a wide range of parameter values that can yield similar dilation rates. To further test the consistency of our model we consider the evolution of clinically measurable mechanical parameters, i.e. the maximum arterial strain $\varepsilon_{\max}$, the pressure strain elastic modulus, E_p and the stiffness parameter γ (see Eqs. 25–27 for definitions); note, the initial physiological values of these parameters are $\varepsilon_{\mathrm{MAX}}(t = 0) = 0.13$, $E_p(t = 0) = 0.4 \times 10^5$ N/m^2 and $\gamma(t = 0) = 3$ respectively. The values of these parameters in our model of a developed AAA are compared with Lanne et al. (1992) clinical study of 37 males, of mean age 74, all of whom suffered from AAAs of mean diameter 41.6 ± 14 mm. To make a quantitative comparison with Lanne et al.'s study we consider the values predicted by our model when the diameter of our model of an AAA is equal to the average of Lanne et al.'s study, i.e. $D_{\mathrm{SYS}} = 41.6\,mm$, for the five parameter sets that give rise to an aneurysm of diameter 45 mm at $t = 10$, namely $(\alpha_H, \beta) = (0.1, 950)$, $(0.5, 195)$, $(2, 25)$, $(3, 10)$ and (6, 0). Our AAA model predicts max diameter strain, $0.015 < \varepsilon_{\mathrm{MAX}} < 0.025$, pressure–strain elastic modulus $1.7 \leq E_p \leq 3 \times 10^5$ N/m^2 and stiffness parameter $16 \leq \gamma \leq 30$. These values are broadly consistent with Lanne et al. (1992) study; the average values they obtained were $\varepsilon_{\mathrm{MAX}} = 0.023 \pm 0.012$, $E_p = 5.04 \pm 2.53(10^5 \mathrm{N/m^2})$ and $\gamma = 34.9 \pm 25.5$.

The increase in stiffness predicted by our model correlates with the decrease in elastin content and increase in collagen content within the arterial wall as the AAA develops. Note that our model predicts values of E_p and γ lower than the mean values observed by Lanne et al. (1992). This may be attributed to the fact that our model does not include effects such as the calcification of the arterial wall, or formation of atherosclerotic plaques, which would act to increase the stiffness further. Also we assume constant, diastolic and systolic pressures in the range 80–120 mmHg whereas the individuals in Lanne et al. (1992) study had a mean blood pressure range from 80 to 150 mmHg.

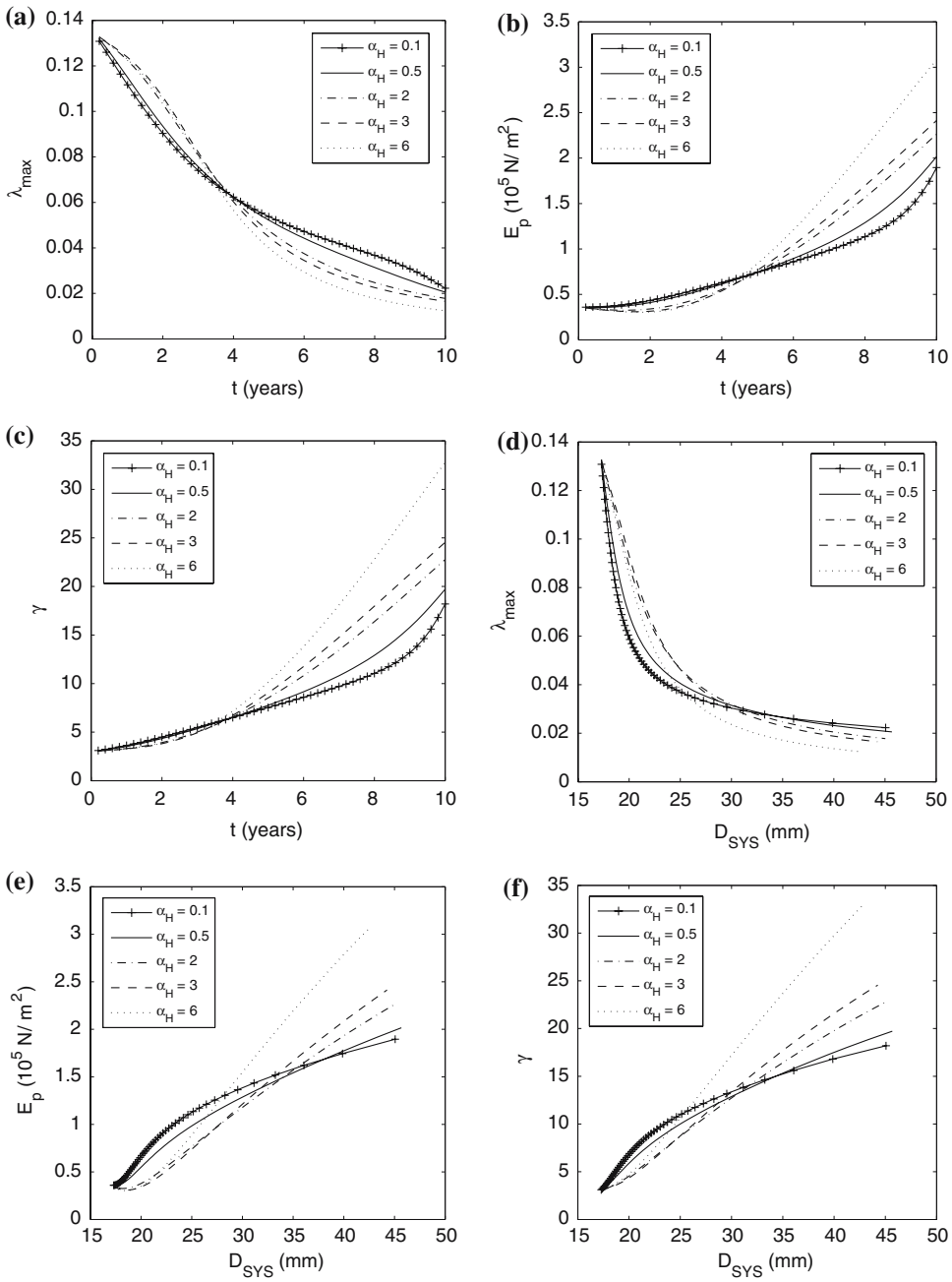

Fig. 11 Various combinations of α_H, β can be chosen to yield an aneurysm of physiological dimensions at $t = 10$, (see Fig. 6) **a** illustrates the evolution of the compliance, $\varepsilon_{\max}$, **b** the evolution of the pressure–strain elastic modulus, E_p and **c** the evolution of the stiffness γ with respect to time. As a function of time: **a** The maximum arterial strain $\varepsilon_{\max}$ decreases exponentially from 13 to 2% **b** the pressure strain elastic modulus, E_p, increases exponentially from 0.4 to approximately 2–3, **c** the stiffness γ increases nonlinearly from 3 to a range of values between 17 and 33. **d** illustrates the evolution of the compliance, $\varepsilon_{\max}$, **e** the evolution of the pressure–strain elastic modulus, E_p and **f** the evolution of the stiffness γ with respect to the systolic diameter. As a function of the arterial diameter, **d** the maximum arterial strain decreases rapidly, E_p **e** and γ f increase nonlinearly

In reality, AAAs may have linear or accelerating expansion, "growth spurts" followed by periods of stasis, or even reduce in size (Brady et al. 2004). Of course, such features of AAA growth could be modelled by adopting more elaborate functional forms for the degradation of elastin. However, whilst this may, seemingly produce more realistic computational simulations of AAA development; at this stage, it would complicate the modelling unnecessarily and not yield further understanding of the aetiology of the disease. Moreover, the functional form of the spatial and temporal degradation is unknown: mathematical models require guidance from physiological studies.

Our AAA model assumes that the distribution of the fibre undulation does not change as the aneurysm develops. This is unlikely, however it would be an unnecessary complication of the model at this stage to address this, particularly given that there is no clinical data available to guide its development. However, future developments of this model may benefit from constitutive models that account for the distribution of the waviness of the collagen fibres in the arterial wall, e.g. Zulliger et al. (2004), or implementing a collagen fibre population model such as that proposed by Sacks (2003) or Sverdlik and Lanir (2002). We also do not account for the dispersion of the fibres about a mean orientation in this paper.

However, a constitutive model that can model fibre dispersion has been recently developed by Gasser et al. (2006). This has been implemented into our remodelling framework; preliminary results show that increased fibre dispersion gives rise to reduced growth rates.

This model assumes the fibre angles are constant relative to the undeformed reference configuration. This naturally implies there is an implicit realignment of the fibres (with respect to the deformed configuration of the tissue) towards directions of increasing principal stretch as the aneurysm develops. There is some justification for approach. Fibroblasts crawl along the existing extra-cellular matrix thus the orientation in which they deposit and degrade collagen is partly dependent on the existing extracellular matrix structure (Dallon and Sherratt 1998). However, fibroblasts are sensitive to their mechanical environment and may attempt to reorientate leading to remodelling of the fibre alignment. Given that the arterial wall in an AAA is comprised largely of collagen, it is important to address how the collagen structure remodels to accurately predict stress distributions and future growth.

This mathematical model uses a linear differential equation to simulate the remodelling effects of fibre deposition and degradation in altered configurations. Remodelling of the collagen fibre density is assumed to be driven by deviations in the strain from an equilibrium value. This relatively simplistic approach is able to predict changes in material and mechanical parameters broadly consistent with clinical observations. However, the cells that synthesise new proteins and produce matrix degrading enzymes within the arterial wall, i.e. fibroblast, smooth muscle and endothelial cells, have not been explicitly represented. Moreover, mechanical stimuli acting on the cells within the arterial wall, e.g. wall shear stress and the frequency/magnitude of cyclic stretching are not accounted for. It is known that the wall shear stress (Chien 2007) and cyclic stretch can profoundly modulate vascular cell processes (Cummins et al. 2007), and thus a more sophisticated modelling approach may be required. In fact, a simple development of this model would be to assume:

'the number of fibroblasts in the arterial tissue is dependent on the mass of collagen that it has to maintain.'

Consequently, given that it is the fibroblasts that deposit collagen fibres, the rate of increase of the collagen density should be dependent on the density of fibroblasts in the arterial wall, or equivalently by the above hypothesis, the density of collagen in the arterial wall. Hence it may be more appropriate to adopt a natural exponential growth law of the form:

$$\frac{\partial n_J}{\partial t} = \beta n^z (E_J^{\mathrm{C}} - E_{\mathrm{A}}), \tag{20}$$

where $z = 1$. Preliminary analysis show that this yields an aneurysm that stabilises in size even if all elastinous constituents are degraded. We tentatively suggest the case $z = 1$ may represent optimum remodelling, whilst $z = 0$ (the case considered in this paper) leads to progressive enlargement of the AAA, and the physiological case may lie anywhere between these extremes, i.e. $0 \leq z \leq 1$. Alternative functional forms to address the remodelling of the collagen density will be explored in subsequent research.

5 Conclusions

The model developed here is the first and to date only mathematical model to consider the evolution of AAA. Our model evolves from a physiologically realistic model of the healthy abdominal aorta and predicts changes in mechanical parameters consistent with experimental observations (Lanne et al. 1992). This gives support to the suitability of our remodelling assumptions and parameters.

The current criterion for the rupture of an AAA is a statistical measure calculated from its diameter. The incorporation of additional patient-specific parameters into the criterion may reduce the uncertainty associated with predicting rupture. Our model illustrates the potential for mathematical models to predict changes in mechanical properties of aneurysms. We conclude that mathematical models of aneurysm growth have the potential to be useful, noninvasive diagnostic tools and thus merit further development.

Acknowledgments We acknowledge the Harwell Software Library (http://www.hsl.ac.uk) for granting UK academics the free use of its FORTRAN subroutines in non-commercial applications. MA38 was employed to solve the linear system that arises in the Newton iteration, which is required to update the deformation at successive time steps.

References

Alberts B, Bray D, Lewis J, Raff M, Roberts K, Watson JD (1994) Molecular biology of the cell. 4th edn. Garland Publishing, Ypsilanti

Armentano R, Barra J, Levenson J, Simon A, Pichel R (1995) Arterial wall mechanics in conscious dogs: assessment of viscous, inertial and elastic moduli to characterize aortic wall behaviour. Circ Res 76(3):468–478

Baek S, Rajagopal KR, Humphrey JD (2006) A theoretical model of enlarging intracranial fusiform aneurysms. J Biomech Eng 128(1):142–149

Brady AR, Thompson SG, Fowkes GR, Greenhalgh RM, Powell JT (2004) Abdominal aortic aneurysm expansion risk factors and time intervals for surveillance. Circulation 100:16–21

Carmo M, Colombo L, Bruno A, Corsi FRM, Roncoroni L, Cuttin MS, Radice F, Mussini E, Settembrini PG (2002) Alteration of elastin, collagen and their cross-links in abdominal aortic aneurysms. Eur J Vasc Endovasc Surg 23:543–549

Chien S (2007) Mechanotransduction and endothelial cell homeostasis: the wisdom of the cell. Am J Physiol Heart Circ Physiol 292:H1209–H1224

Cummins PM, VonOffenberg Sweeney N, Kileen MT, Birney YA, Redmond EM, Cahill PA (2007) Cyclic strain-mediated matrix

metalloproteinase regulation within the vascular endothelium: a force to be reckoned with. Am J Physiol Heart Circ Physiol 292:H28–H42
Davies MJ (1998) Aortic aneurysm formation: Lessons from human studies and experimental models. Circulation 98:193–195
Dallon J, Sherratt JA (1998) A mathematical model for fibroblast and collagen orientation. Bull Math Biol 60:101–130
Elger D, Blackketter D, Budwig R, Johansen K (1996) The influence of shape on the stresses in model abdominal aortic aneurysms. J Biomech Eng 118:326–332
Gasser TC, Ogden RW, Holzapfel GA (2006) Hyperelastic modelling of arterial layers with distributed collagen fibre orientations. J R Soc Interface 3:15–35
Gleason RL, Humphrey JD (2004) A mixture model of arterial growth and remodeling in hypertension: altered muscle tone and tissue turnover. J Vas Res 41:352–363
Gleason RL, Humphrey JD (2005) Effects of a sustained extension on arterial growth and remodeling: a theoretical study. J Biomech 38(6):1255–1261
Gleason RL, Taber LA, Humphrey JD (2004) A 2-D model of flow-induced alterations in the geometry, structure and properties of carotid arteries. ASME J Biomech Eng 126:371–381
Gundiah N, Ratcliffe MB, Pruitt LA (2007) Determination of strain energy function for arterial elastin: experiments using histology and mechanical tests. J Biomech 40:586–594
Hansen KA, Weiss JA, Barton JK (2002) Recruitment of tendon crimp with applied tensile strain. ASME J Biomech Eng 124:72–77
He CM, Roach M (1993) The composition and mechanical properties of abdominal aortic aneurysms. J Vasc Surg 20(1):6–13
Heil M (1996) The stability of cylindrical shells conveying viscous flow. J Fluids Struct 10:173–196
Holzapfel GA (2006) Determination of material models for arterial walls from uniaxial extension tests and histological structure. J Theor Biol 238:290–302
Holzapfel GA, Gasser TC, Ogden RW (2000) A new constitutive framework for arterial wall mechanics and a comparative study of material models. J Elast 61:1–48
Holzapfel GA, Gasser TC, Stadler M (2002) A structural model for the viscoelastic behaviour of arterial walls: continuum formulation and finite element analysis. Eur J Mech A Solids 21:441–463
Holzapfel GA, Sommer G, Auer M, Regitnig P, Ogden RW (2007) Layer-specific 3D residual deformations of human aortas with non-atherosclerotic intimal thickening. Ann Biomed Eng 35(4): 530–545
Humphrey JD (1999) Remodelling of a collagenous tissue at fixed lengths. J Biomech Eng 121:591–597
Humphrey JD (2002) Cardiovascular solid mechanics, Springer, Berlin
Humphrey JD, Rajagopal KR (2002) A constrained mixture model for growth and remodeling of soft tissues. Math Model Methods Appl Sci 12:407–430
Humphrey JD, Rajagopal KR (2003) A constrained mixture model for arterial adaptations to a sustained step-change in blood flow. Biomech Model Mechanobiol 2:109–126
Kroon M, Holzapfel GA (2007) A model for saccular cerebral aneurysm growth by collagen fibre remodelling. J Theor Biol (in press)
Lanne T, Sonesson B, Bergqvist D, Bengtsson H, Gustafsson D (1992) Diameter and compliance in the male human abdominal aorta: influence of age and aortic aneurysm. Eur J Vasc Surg 6:178–184
Langewouters GJ, Wesseling KH, Goehard WJA (1984) The static elastic properties of 20 abdominal aortas in vitro and the parameters of a new model. J Biomech 17:425–435
Learoyd BM, Taylor MG (1966) Alterations with age in the viscoelastic properties of human arterial walls. Circ Res 18:278–292
Mohan D, Melvin JW (1982) Failure properties of passive human aortic tissue. II- Biaxial tension tests. J Biomech 16(1):31–44
Nissen R, Cardinale GJ, Udenfriend S (1978) Increased turnover of arterial collagen in hypertensive rats. Proc Natl Acad Sci USA Med Sci 75(1):451–453
Ogden RW, Schulze-Bauer CAJ (2000) Phenomenological and structural aspects of the mechanical response of arteries. Mech Biol AMD-242, BED-46, New York pp 125–140
Powell JT, Brady AR (2004) Detection, management and prospects for the medical treatment of small abdominal aortic aneurysms. Arterioscler Throm Vasc Biol 24:241–245
Raghavan ML, Vorp DA (2000) Toward a biomechanical tool to evaluate rupture potential of abdominal aortic aneurysm: identification of a finite strain constitutive model and evaluation of its applicability. J Biomech 33:475–482
Raghavan ML, Webster M, Vorp DA (1999) Ex-vivo bio-mechanical behavior of AAA: assessment using a new mathematical model. Ann Biomed Eng 24:573–582
Raghavan ML, Kratzberg J, De Tolosa EMC, Hanaoka MM, Walker P, Da Silva ES (2006) Regional distribution of wall thickness and failure properties of human abdominal aortic aneurysm. J Biomech 39:3010–3016
Rachev A, Greenwald SE (2003) Residual strains in conduit arteries. J Biomech 36(5):661–670
Sacks MS (2003) Incorporation of experimentally derived fiber orientation into a structural constitutive model for planar collagenous tissues. ASME J Biomech Eng 125:280–287
Shadwick R (1999) Mechanical design in arteries. J Exp Biol 202:3305–3313
Shimizu K, Mitchell RN, Libby P (2006) Inflammation and cellular immune responses in abdominal aortic aneurysms. Arterioscler Thromb Vasc Biol 26:987–994
Sonneson B, Lanne T, Vernersson E, Hansen F (1994) Sex difference in the mechanical properties of the abdominal aorta in human beings. J Vasc Surg 20:959–969
Stalhand J, Klarbring A, Karlsson M (2004) Towards in vivo aorta material identification and stress estimation. Biomech Model Mechanobiol 2:169–186
Stalhand J, Klarbring A (2005) Aorta in vivo parameter identification using an axial force constraint. Biomech Model Mechanobiol 3:191–199
Stergiopulos N, Vullièmoz S, Rachev A, Meister J, Greenwald S (2001) Assessing the homogeneity of the elastic properties and composition of the pig aortic media. J Vasc Res 38(3):237–246
Sverdlik A, Lanir Y (2002) Time dependent mechanical behaviour of sheep digital tendons, including the effects of preconditioning. ASME J Biomecl Eng 124:78–84
Takamizawa K, Hayashi K (1987) Strain energy density function and uniform strain hypothesis for arterial mechanics. J Biomech 20(1):7–17
Van de Geest JP, Sacks MS, Vorp DA (2006) The effects of aneurysm on the biaxial mechanical behaviour of human abdominal aorta. J Biomech 39:1324–1334
Vardulaki KA, Prevost TC, Walker NM, Day NE, Wilmink ABM, Quick C, Ashton H, Scott R (1998) Growth rates and risk of rupture of abdominal aortic aneurysms. Br J Surg 85:1674–1680
Vorp DA (2007) Review: biomechanics of abdominal aortic aneurysm. J Biomech 40:1887–1902
Watton PN (2002) Mathematical modelling of the abdominal aortic aneurysm, PhD Thesis, Dept. of Applied Mathematics, University of Leeds, Leeds
Watton PN, Heil M, Hill NA (2004) A mathematical model for the growth of the abdominal aortic aneurysm. Biomech Model Mechanobiol 3(2):98–113
Wempner G (1973) Mechanics of solids. McGraw-Hill, New York
Wilmink WBM, Quick CRG, Hubbard CS, Day NE (1999) The influence of screening on the incidence of ruptured abdominal aortic aneurysms. J Vasc Surg 30(2):203–208

Wuyts FL, Vanhuyse VJ, Langewouters GJ, Daecraemer WF, Raman ER, Buyle S (1995) Elastic properties of human aortas in relation to age and atherosclerosis: a structural model. Phys Med Biol 40:1577–1597

Zulliger MA, Montorzi G, Stergiopulos N (2004) A strain energy function for arteries accounting for wall composition and structure. J Biomech 37:989–1000